

Fibrous Composite with Threshold Strength in Three Dimensions

X.H. JIN, L. GAO*, J. SUN, L.H. GUI

The State Key Laboratory on High Performance Ceramics and Superfine Microstructures, Shanghai Institute of Ceramics, Shanghai, China, 200050

*e-mail: liangaoc@online.sh.cn

Abstract

In the present work, a fibrous composite consisting of square fibers separated with thin compressive layer is designed. Due to the crack arresting effect of the compressive layer, this composite is expected to show three-dimensional threshold strengths corresponding to applied stresses in the direction perpendicular to the fiber side face and parallel to the fiber central axis, respectively. In accordance with the above designing concept, $\text{Si}_3\text{N}_4/\text{TiN}$ fibrous composites with distinctive threshold strengths were readily prepared through a simple double-laminating procedure. It is found that the threshold strengths increase with the TiN content in the fiber; and for the same material, its axial threshold strength is larger than the radial one. The fundamental reasons for that are investigated.

Keywords: Fibrous composite, Threshold strength, Crack arresting, Si_3N_4 , TiN

KOMPOZYT WŁÓKNISTY Z WYTRZYMAŁOŚCIĄ PROGOWĄ W TRZECH WYMIARACH

W prezentowanej pracy zaprojektowano kompozyt włóknisty składający się z włókien o przekroju kwadratowym, rozdzielonych cienką warstwą zawierającą naprężenia ściskające. Z powodu efektu zatrzymywania pęknięcia od kompozytu tego oczekuje się, że pokaże trójwymiarową wytrzymałość progową odpowiadającą zastosowanym naprężeniom w kierunku odpowiednio prostopadłym do powierzchni czołowej włókna i równoległym do jego centralnej osi włókna. Zgodnie z koncepcją projektową bez trudu przygotowano kompozyty włókniste $\text{Si}_3\text{N}_4/\text{TiN}$ za pomocą prostej procedury podwójnego laminowania. Stwierdza się, że wytrzymałości progowe zwiększają się wraz z zawartością TiN we włóknie, i dla tego samego materiału, jego osiowa wytrzymałość progowa jest większa niż promieniowa. Zbadano zasadnicze powody występowania takiego stanu.

Słowa kluczowe: kompozyt włóknisty, wytrzymałość progowa, zatrzymywanie pęknięcia, Si_3N_4 , TiN

1. Introduction

The strength of ceramics is highly sensitive to the flaw size due to its brittle nature. This makes the strength of a specific ceramic component unpredictable, which seriously affects its using reliability. In order to solve the problem, many measures have been taken to improve the toughness of ceramics [1-4] but the effect is relatively limited. Till now, low reliability associated with poor toughness has still posed an obstacle for the wide application of ceramics in structural fields.

Recently, Lange and his colleagues have found that a composite composed of an alternately laminated tensile thick layer and a compressive thin layer could show a threshold strength due to the crack arresting effect of the latter layer [5-8]. This discovery opens a new way to solve reliability problem of ceramics. It allows the engineer to design structural components with the knowledge that the component will not fail below the threshold strength, as claimed by Rao [5]. However, this kind of laminar composite has an inborn shortcoming. That is, restricted by its laminar structure, it exhibits threshold strength only under a load parallel to the

layers. The strong dependence of threshold strength on load direction is undesirable for the application of the material.

In the present work, a fibrous composite is designed as shown in Fig. 1. This material consists of square fibers separated with thin interlayer of lower thermal expansion coefficient. Suppose that failure is controlled by the flaws within the fibers, then two threshold strengths can be expected in this material as a result of the crack arresting effect of the compressive stress within the interlayer. These threshold strengths correspond to the applied stresses in the direction perpendicular to the fiber side face and parallel to the fiber central axis, and are denoted as radial and axial

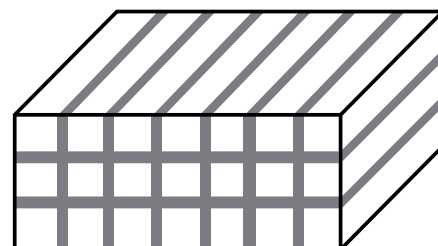


Fig. 1. Schematic illustration showing the architecture of the fibrous composite.

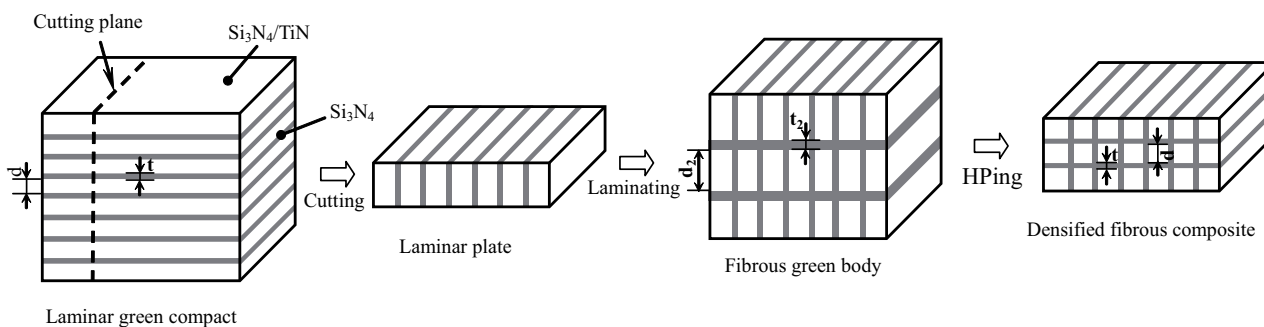


Fig. 2. Flow chart showing the fabrication procedure of $\text{Si}_3\text{N}_4/\text{TiN}$ fibrous composite.

threshold strength, respectively. Therefore, the composite shows threshold strengths in three dimensions, and the load direction sensitivity of threshold strength is greatly reduced in comparison with a laminar composite. This gives a greater flexibility for a reliable structural component design.

2. Experimental

To testify the above designing concept, fibrous composites composed of $\text{Si}_3\text{N}_4/\text{TiN}$ square fibers and Si_3N_4 thin layer were fabricated. These composites were denoted as ST-30, ST-35 and ST-40 according to the TiN content of the fiber, which were 30, 35 and 40 vol.%, respectively. We hope that the thermal mismatch between the $\text{Si}_3\text{N}_4/\text{TiN}$ fiber and the Si_3N_4 thin layer will lead to the origin of compressive stresses within the latter, and thus the appearance of three dimensional threshold strengths in the composite.

Fig. 2 shows the flow chart of the fabrication procedure. First, a laminar green compact composed of alternating $\text{Si}_3\text{N}_4/\text{TiN}$ thick layer and Si_3N_4 thin layer was fabricated by laminating $\text{Si}_3\text{N}_4/\text{TiN}$ and Si_3N_4 sheets that were prepared by the tap casting method. Then the laminar compact was cut into plates of designated thickness in the direction perpendicular to the layers, softened in ethanol vapor and laminated again with a second set of Si_3N_4 sheet. After debinderig in vacuum at 850°C , the green compact formed was hot pressed in a size-fitted graphite mould at 1800°C for 1 h under 30 MPa. During hot pressing, the restriction from the mould wall allowed the sample only to shrink uniaxially along the direction of the applied load.

In the end, a fibrous composite composed of square fibers separated with thin compressive layer was obtained if the thickness of the plate and the second set of Si_3N_4 sheet in the green compact were precisely controlled.

The sintered samples were cut into bars of $3\text{ mm} \times 4\text{ mm} \times 35\text{ mm}$, mirror polished, then an artificial crack aligning in the direction perpendicular to the Si_3N_4 compressive layer was produced on the sample surface by the Vickers indentation method. This artificial crack was located in either the center of the fiber's cross section region or the center of the

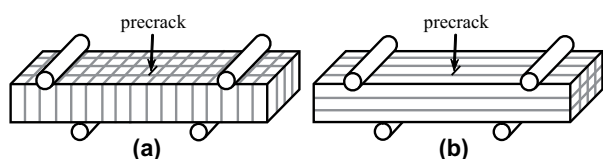


Fig. 3. Schematic illustration showing the measurement of threshold strength by the four-point bending method: a) radial, and b) axial.

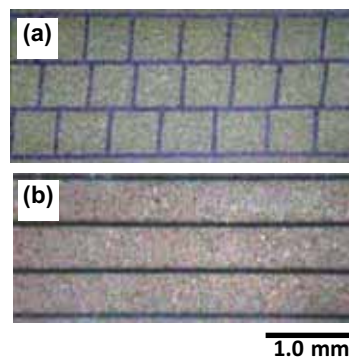


Fig. 4. Optical micrographs of the ST-30 composite: a) in direction along the central axis of the fiber, and b) perpendicular to the fiber's side face.

fiber's side face, depending on either the radial or the axial threshold strength would be tested (Fig. 3). The residual strength of the precracked sample was measured in a four-point bending at a crosshead speed of 0.05 mm/min. The microstructure was characterized with optical and scanning electron microscopy.

3. Results and discussion

Fig. 4 shows the typical optical images of the fibrous composite ST-30. The $\text{Si}_3\text{N}_4/\text{TiN}$ fibers in the material show a nearly perfect square cross section with thin Si_3N_4 interlayer among them, the fiber diameter and the interlayer thickness in it are about $450\ \mu\text{m}$ and $54\ \mu\text{m}$, respectively. No significant deviation from the designed architecture is observed except some mismatch in the position of the Si_3N_4 interlayer. The fibrous composites ST-35 and ST-40 have nearly the same architecture as ST-30, although they are not shown here. This indicates a good reproducibility of the fabrication technique.

Figs. 5a and 5b show the variation of residual strength with the precrack length during the radial and axial threshold strength testing of the fibrous composite ST-30. In addition, for the purpose of comparison, the residual strength of a precracked $\text{Si}_3\text{N}_4/\text{TiN}$ monolithic composite containing 30 vol.% TiN but without the Si_3N_4 interlayer is also reported in Fig. 5a. It is found that the residual strength of the $\text{Si}_3\text{N}_4/\text{TiN}$ monolithic composite is strongly sensitive to the precrack size, and gradually decreases with an increase in the precrack length, which is typical for a brittle material. Conversely, the residual strengths of the fibrous composite show little variation with the precrack length and distinctive threshold strength phenomena are observed for both the

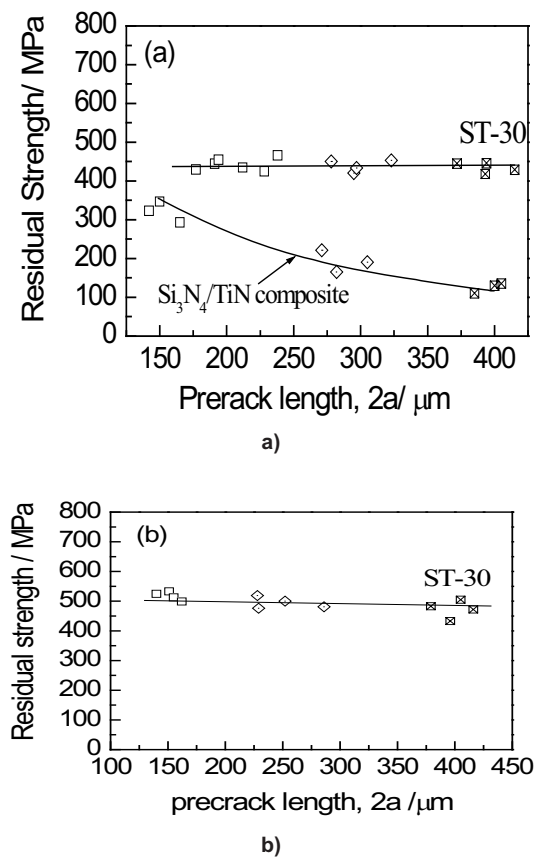


Fig. 5. Plots of the residual strength versus precrack length for ST-30 fibrous composite during (a) radial and (b) axial threshold strength testing, using precracks made at indenter loads of 49N (\square), 98N (\diamond) and 196 N (\boxtimes). For comparison, the residual strength of a conventional $\text{Si}_3\text{N}_4/\text{TiN}$ composite containing 30 vol.% TiN is also reported in plot (a).

radial and the axial threshold strength testing, because of the crack arresting effect of the Si_3N_4 compressive interlayer as shown below.

Figs. 6a–6d show the optical micrographs of a precracked ST-40 specimen after loading at applied stresses of 300–480 MPa during the radial threshold strength testing. The precrack in this specimen is originally 210 μm in length and located in the center of the fiber cross section. After loading with externally applied stress, the precrack penetrates straight into the Si_3N_4 layer, and the penetration depth increases with an increase in the applied stress before it penetrates through the Si_3N_4 layer at 503 MPa, where catastrophic failure occurs. This stable crack growth behaviour is a clear evidence of the crack arresting effect of the Si_3N_4 compressive layer, although the crack stabilizing effect of the indentation field associated with the precrack cannot be completely excluded. The previous research found that an indented crack could grow to about 2.5 times of its initial size without losing stability due to the crack stabilizing effect of the indentation field, and the residual strength (σ_r) decreased with the indenter load (P), following $\sigma_r \propto P^{-1/3}$ [9]. However, the residual strength is nearly independent of the indenter load for the present fibrous composite (see Fig. 5), which implies that the crack stabilizing effect of the indentation field is much weaker in comparison with that of the compressive stresses within the Si_3N_4 layer. Hereby, it can be concluded that it is the crack

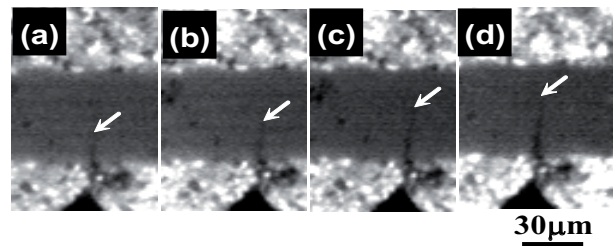


Fig. 6. Optical micrographs of a precracked ST-40 sample taken after loading at stresses of: a) 300 MPa, b) 360 MPa, c) 420 MPa, and d) 480 MPa during radial threshold strength testing.

arresting effect of the compressive Si_3N_4 layer that mainly accounts for the stable crack growth and the appearance of threshold strength phenomena in the composite.

Fig. 7 shows the measured threshold strengths of the ST-30, ST-35 and ST-40 fibrous composites. The radial and axial threshold strengths increase proportionally with the TiN content in the fiber, because of the increase in the compressive stress within the Si_3N_4 interlayer, which leads to a stronger crack arresting effect. For the same material, its axial threshold strength is generally 50–60 MPa higher than the radial one. The specific reason for such a difference between the radial and axial threshold strength is not quite clear, and is most likely related with the difference in crack configuration at the failure point during the threshold strength testing. Restricted by the Si_3N_4 compressive layers, the surface indentation crack will extend deeply into the material without significant transverse crack growth during the radial threshold strength testing as observed by Rao in a laminar composite [7]. This makes it develop into a slit crack before the failure of the material. In contrast, the surface indentation crack evolves into a square plane crack that is three-side bounded with Si_3N_4 compressive layer prior to failure of the material during the axial threshold strength testing. Since the stress intensity factor of a square plane crack is much smaller than that of a slit crack [10], a higher applied stress is needed for the former crack to break through the Si_3N_4 compressive layer, which results in a higher axial threshold strength.

Till now, the existence of threshold strengths in the $\text{Si}_3\text{N}_4/\text{TiN}$ fibrous composite has been unambiguously testified. But in comparison with the intrinsic strength of the material (900–1100 MPa), the threshold strengths are much lower. Therefore, further optimization of the threshold strengths is desired, which can be realized by increasing the compressive stress within the Si_3N_4 interlayer and adjusting the structural

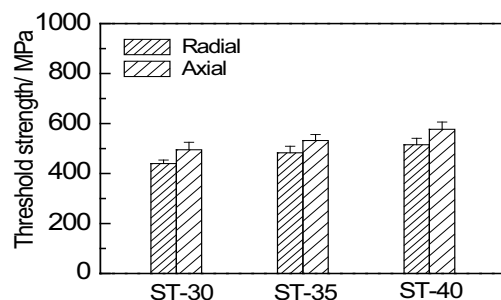


Fig. 7. The measured radial and axial threshold strength of the $\text{Si}_3\text{N}_4/\text{TiN}$ fibrous composites.

parameters of the material. As to the latter, a reduction in the fiber diameter while keeping the Si_3N_4 interlayer thickness sufficiently small in comparison with the fiber diameter might be a good choice. In this case, the critical crack size for failure is reduced during the threshold strength testing, and accordingly an improvement in the threshold strength should be realized.

4. Conclusions

$\text{Si}_3\text{N}_4/\text{TiN}$ fibrous composites composed of $\text{Si}_3\text{N}_4/\text{TiN}$ square fibers and Si_3N_4 thin compressive interlayer were successfully fabricated. Due to the crack arresting effect of the Si_3N_4 layer, these composites show threshold strengths corresponding to the applied tensile stresses in the direction perpendicular to the fiber side face and parallel to the fiber central axis, respectively. The threshold strengths increase with the TiN content in the fiber, as a result of the increase in the compressive stress within the Si_3N_4 layer. For the same material, its axial threshold strength is larger than the radial one, because of the difference in the crack configuration at the failure point.

Acknowledgements

This research was supported by the natural science foundation of China under grant numbers of 50402006 and 50672112.

References

- [1] Hannink R.H.J., Swain M.V.: „Progress in Transformation Toughening of Ceramics”, *Annu. Rev. Mat. Sci.*, 24, (1994), 359-408.
- [2] Chen I.W., Rosenflanz A.: „A tough SiAlON ceramic based on $\alpha\text{-Si}_3\text{N}_4$ with a whisker-like microstructure”, *Nature*, 389, (1997), 701-704.
- [3] Shen Z.J., Zhao Z., Peng H., Nygren M.: „Formation of tough interlocking microstructures in silicon nitride ceramics by dynamic ripening”, *Nature*, 417, (2002), 266-269.
- [4] Clegg W.J., Kendall K., Alford N.M., Botton T. W., Birchall J.D.: „Simple Way to Make Tough Ceramics”, *Nature*, 347, (1990), 455-457.
- [5] Rao M.P., Sánchez-Herencia A.J., Beltz G.E., McMeeking R.M. Lange F.F.: „Laminar Ceramics That Exhibit a Threshold Strength”, *Science*, 286, (1999), 102-105.
- [6] Rao M.P., Rödel J., Lange F.F.: „Residual Stress Induced R-Curves in Laminar Ceramics That Exhibit a Threshold Strength”, *J. Am. Ceram. Soc.*, 84, (2001), 2722-24.
- [7] Rao M.P., Lange F.F.: „Factors Affecting Threshold Strength in Laminar Ceramic Containing Thin Compressive Layers”, *J. Am. Ceram. Soc.*, 85, (2002), 1222-28.
- [8] Pontin M.G., Rao M.P., Sánchez-Herencia A.J., Lange F.F.: „Laminar Ceramics Utilizing the Zirconia Tetragonal-to-Monoclinic Phase Transformation to Obtain a Threshold Strength”, *J. Am. Ceram. Soc.*, 85, (2002), 3041-48.
- [9] Lawn B.R.: „Fracture of Brittle Solids”, 2nd Ed., Cambridge University Press, (1993), 266-271.
- [10] Murakaki Y.: „Stress Intensity Factors Handbook”, Pergamon Press, New York, (1988), 810-811.

◆

Received 23 April 2010; accepted 8 May 2010